A MODEL OF PRIMATE PHOTORECEPTORS

Hugo R. Gonçalves and Miguel V. Correia
Instituto de Engenharia de Sistemas e Computadores do Porto
Universidade do Porto, Faculdade de Engenharia, Dept. Eng. Electrotécnica e de Computadores
R. Dr. Roberto Frias, 4200-465 Porto, Portugal

Keywords: Retina model, Primate, Adaptation, Bleaching, Photoreceptors, Cone, Rod.

Abstract: As experimental research reveals the biological mechanisms behind the processing done by the retina, complete models of the retina become more and more possible. This paper presents a temporal model of primate photoreceptors inspired by the mechanisms discovered in other species. It implements light adaptation based on pigment bleaching and biochemical reactions. The simulation provides similar results to experiments made in impulse, contrast and sensitivity response curves of primate cones and rods.

1 INTRODUCTION

The body of information resultant from investigating the physiology and anatomy of the mammalian retina has revealed several mechanisms that work together to process visual signals. In contrast, monkey retina, the one most similar to the human retina with the exception of apes, is less examined. Nevertheless, primate and other mammals' retinae seem to process visual signal in the same way (Perlman and Normann, 1998; Masland, 2001).

A model of the primate retina is more desirable than others due to the resemblance to the human retina, which makes it the best candidate for neural prostheses and more adequate to provide input to human visual cortex models.

The first model describing the behaviour of primate photoreceptors and horizontal cells was introduced by (van Hateren, 2005), who compared his model results with experimental results of horizontal cells. van Hateren work continued by adding spatial calculation in the horizontal cell network (van Hateren, 2007) and pigment bleaching in cones (van Hateren and Snippe, 2007). However, the confrontation of results is only done in horizontal cells.

The model presented here was implemented in Matlab Simulink® and is intended to i) simulate primate photoreceptors in time, ii) use biological plausible mechanisms and iii) simple equations with possibility of implementation in hardware. The model implements both cones and rods and light adaptation in cones, in the form of pigment bleaching and biochemical adaptation.

Section 2 describes the model, Section 3 defines the values of the model parameters and their source, Section 4 compares the model results with experimental results of primates and Section 5 concludes the paper.

2 METHODS

The model simulates two types of photoreceptors, cones and rods, in time, in millisecond steps. Photoreceptors transduce light into voltage. Rods are much more sensitive to light than cones, and are responsible for vision under scotopic light levels. Under photopic light, rods saturate and cones adjust their sensitivity and operating point to the ambient light.

2.1 Cones

Although in real retinas, both rods and cones adapt to light, adaptation was only integrated into cones in the model. Two forms of adaptation were implemented: pigment bleaching and calcium-dependent adaptation.

2.1.1 Pigment Bleaching

During absorption of photons, photoreceptor pigment bleaches and induces a chain of reactions that con-

Gonçalves H. and Correia M. (2010).
A MODEL OF PRIMATE PHOTORECEPTORS.
In *Proceedings of the Third International Conference on Bio-inspired Systems and Signal Processing*, pages 277-283
DOI: 10.5220/0002746102770283

verts light into electrical signal. The pigment is then unbleached at a certain rate. Following the conclusions of (Mahroo and Lamb, 2004), human bleaching has slow, rate-limited dynamics. For a certain amount of steady light I, the fraction of unbleached pigment P follows Eq. 1:

$$\frac{\partial P}{\partial t} = \underbrace{\frac{K_m \cdot (1-P)}{K_m + (1-P)} \cdot \frac{1}{\tau_b}}_{\text{recovery}} - \underbrace{\sigma \cdot I \cdot P}_{\text{bleaching}}, \qquad (1)$$

where σ is the cone photosensitivity, τ_b is the recovery time constant and K_m is a constant defining the range in which pigment bleaching is rate-limited. For values of $P \approx 1$, the dynamics of the recovery process reduces to first-order, with time constant τ_b. As P decreases and $1-P$ becomes greater than K_m, the recovery process loses dependence on P and the dynamics become rate-limited. The equivalent light after bleaching is $I_b = I \cdot P$.

Pigment bleaching has the very important role of limiting the amount of photoconversion happening under very bright light. Under such conditions, any increase in light is counteracted in the long-term by the reduction in the fraction of unbleached pigment, and the amount of photoconversion remains the same.

2.1.2 Calcium-dependent Adaptation

The chain of reactions triggered by photon absorption starts by pigment bleaching, which in turn activates the enzyme phosphodiesterase (PDE). This two-stage chain can be modeled by two first-order low-pass filters, converting I_b to PDE^* (activated PDE molecule) with no gain. Each PDE^* hydrolyzes the second messenger *cGMP* (Cyclic Guanosine Monophosphate) at a rate β_{cGMP}, reducing its concentration. The synthesis of *cGMP* is controlled by guanylate cyclase activity (α_{cGMP}). Thus, the variation of *cGMP* can be formulated as (Soo et al., 2008)

$$\frac{\partial cGMP}{\partial t} = \alpha_{cGMP} - \beta_{cGMP} \cdot PDE^* \cdot cGMP. \qquad (2)$$

The cGMP controls channels in the cone outer segment (more cGMP, more channels open). The channels regulate the light-sensitive circulating current into the cone inner segment (Perlman and Normann, 1998). In vertebrates, light adaptation is controlled by Ca^{2+} concentration in photoreceptor outer segment (Fain et al., 2001; Koutalos and Yau, 1996; Perlman and Normann, 1998). As the light-sensitive channels are closed with light, the Ca^{2+} concentration (Ca_C) is reduced proportionally (Koutalos and Yau, 1996) ($Ca_C \propto cGMP$). This reduction leads to a) disinhibiton of guanylate cyclase activity, accelerating the rate of cGMP synthesis and b) reduction in PDE activation rate, diminishing cGMP hydrolysis (Koutalos and Yau, 1996). Both effects raise the equilibrium cGMP concentration. Thus, two negative feedbacks are used to control light adaptation. Therefore, the cone adaptation is formulated as

$$\begin{aligned} \frac{\partial cGMP}{\partial t} &= \alpha_{cGMP} \cdot \eta(Ca_C) \qquad (3) \\ &\quad -\beta_{cGMP} \cdot cGMP \cdot (PDE^* \cdot \gamma(Ca_C) + 1). \end{aligned}$$

The + 1 term corresponds to the current under dark conditions (dark current). Eq. 3 states that under steady luminance (constant Ca^{2+} concentration), the response to a contrast step will be

$$cGMP = \frac{\alpha_{cGMP} \cdot \eta(Ca_C)}{\beta_{cGMP} \cdot (PDE^* \cdot \gamma(Ca_C) + 1)}. \qquad (4)$$

This is the same expression as the Michaelis relation $cGMP = cGMP_{max} \cdot I_0/(I + I_0)$, where $I_0 = 1/\gamma(Ca_C)$, $I = PDE^*$ and $cGMP_{max} = \alpha_{cGMP} \cdot \eta(Ca_C)/\beta_{cGMP}$. The relation $\eta(Ca_C)$ was modified from (Koutalos and Yau, 1996) and $\gamma(Ca_C)$ was found to give the best fit when a linear relation is established:

$$\gamma(Ca_C) = [\gamma_a Ca_C + \gamma_b]^+ \qquad (5)$$

$$\eta(Ca_C) = \eta_{max} \frac{1}{Ca_C + \eta_h}, \qquad (6)$$

where γ_a and γ_b are constants, $[\cdot]^+$ is equivalent to $\max(\cdot, 0)$, and η_{max} is the maximum value of η, when $Ca_C \ll \eta_h$. Reducing Ca^{2+} concentration a) decreases γ (because γ_a is positive) and shifts the half-saturation constant I_0 to higher values and b) increases η and consequently $cGMP_{max}$. For the sake of simplicity, Ca_C is equal to *cGMP*.

2.1.3 Inner Segment

The inner segment of the photoreceptors integrate circulating current into the membrane potential, much like any neuron does. The conductance-based model of the neuron (Hodgkin and Huxley, 1952) was used here. Briefly, the neuron is composed by a group of conductances, each pulling the membrane potential to its reversal potential. A leakage current pulls the neuron potential to rest. In its general form, the membrane potential V is defined as

$$C\frac{\partial V}{\partial t} = G_{ex}(V_{ex} - V) + G_{in}(V_{in} - V) + G_{leak}(V_{leak} - V), \qquad (7)$$

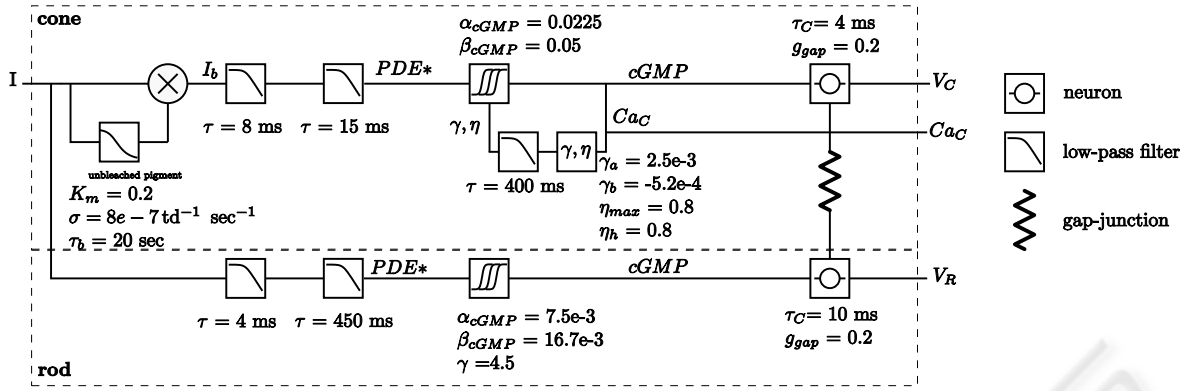

Figure 1: Model of photoreceptors.

where C is the membrane capacitance, G_{ex} and V_{ex} are the excitation conductance and reversal potential, G_{in} and V_{in} are the inhibition conductance and reversal potential, and G_{leak} and V_{leak} are the fixed leakage conductance and resting potential.

In order to simplify parameter choice, conductance and capacitance values were normalized to G_{leak}, i.e.,

$$\tau_C \frac{\partial V}{\partial t} = g_{ex}(V_{ex} - V) + g_{in}(V_{in} - V) + (V_{leak} - V), \tag{8}$$

where

$$g_{ex} = \frac{G_{ex}}{G_{leak}}, g_{in} = \frac{G_{in}}{G_{leak}}, \tau_C = \frac{C}{G_{leak}}.$$

In the rest of the article, when referring to conductances, they are normalized. Unless stated otherwise, $V_{leak} = -72\,\text{mV}$, $V_{in} = -80\,\text{mV}$ and $V_{ex} = 0\,\text{mV}$.

Additionaly, neurons can have gap-junction conductances. This conductance is the electrical coupling between neurons close enough to each other, that ions are transferred by diffusion to the neuron with a lower concentration. Gap-junctions can be made with neurons of the same (homotypic) or different types (heterotypic coupling). For heterotypic coupling, the gap-junction conductance can be added to Eq. 8 in the following way:

$$\tau_C \frac{\partial V}{\partial t} = \sum_x g_x(V_x - V) + g_{gap}(V_n - V). \tag{9}$$

g_{gap} is the strength of the junction (higher values mean more diffusion) and V_n is the membrane potential of the adjacent neuron of the other type. For reciprocal conductances, this term should be added to the equations of both neurons. Cones make reciprocal gap-junctions with rods (Hornstein et al., 2005; Schneeweis and Schnapf, 1999).

Cone inner segment model was inspired by the simple, but effective work of (Baylor et al., 1974), in which the inner segment is composed of a leakage, a light-sensitive (g_i) and a voltage-dependent (g_f) currents. g_i bears a close resemblance to the steady-state form of cGMP (Eq. 4). g_f is a sigmoidal function of the cone voltage. This conductance is named here g_h to demark that it is equivalent to the hyperpolarization-activated current, and is expressed as

$$g_h(V) = \frac{g_{h_{max}}}{1 + \exp\left(\frac{V - V_f}{k}\right)}, \tag{10}$$

followed by a low-pass filter with time constant τ_h. The reversal potential V_h of this conductance was considered to be -30 mV (Bader et al., 1982).

In sum, the cone equation is

$$\begin{aligned}\tau_C \frac{\partial V}{\partial t} &= cGMP \cdot (0 - V) + g_h \cdot (V_h - V) \\ &\quad + (V_{leak} - V) + g_{gap} \cdot (V_{rod} - V),\end{aligned} \tag{11}$$

with $cGMP$ ruled by Eq. 3, g_h ruled by Eq. 10 and V_{rod} is the potential of the coupled rod.

2.2 Rods

Rods have very slow dynamics, which allows them to integrate more light, becoming more sensitive.

For simplification, light adaptation was not implemented in rods. In that sense, pigment bleaching is ignored and the cGMP synthesis and hydrolysis are not controled by calcium concentration, changing Eq. 3 to

$$\frac{\partial cGMP}{\partial t} = \alpha_{cGMP} - \beta_{cGMP} \cdot cGMP \cdot (PDE^* \cdot \gamma + 1). \tag{12}$$

The γ factor is a constant for rods, and amplifies the hydrolysis of *cGMP* by $PDE*$. The hyperpolarization-activated conductance g_h also exists in rods.

In sum, the rod equation is

$$\tau_C \frac{\partial V}{\partial t} = cGMP \cdot (0-V) + g_h \cdot (V_h - V) + (V_{leak} - V) + g_{gap} \cdot (V_{cone} - V) \quad (13)$$

with *cGMP* ruled by Eq. 12, g_h ruled by Eq. 10 and V_{cone} is the potential of the coupled cone.

3 MODEL PARAMETERS CHOICE

For the pigment bleaching parameters, K_m and τ_b values were taken from (Mahroo and Lamb, 2004) ($K_m = 0.2$, $\tau_b = 20$ sec). The photosensitivity was changed to $\sigma = 8e-7\,\text{td}^{-1}\text{sec}^{-1}$ to be adjusted to the half-bleach intensity of 4.3 log td[1] (Rushton and Henry, 1968; Valeton and van Norren, 1983).

Membrane potentials of macaque cones can range from ≈ -50 mV in the dark, down to -70 mV in response to bright light (Verweij et al., 2003). Considering that $PDE^* = 0$ in the dark (Eq. 3), $\alpha_{cGMP}/\beta_{cGMP}$ ratio was chosen such that maximal cGMP conductance in the dark would cause cones to depolarize to -50 mV ($\eta(Ca_C) = 1$ in the dark). This was achieved with a ratio of 0.45. The individual values are shown adjacent to the symbol in Fig. 1. The values of the first time constants were adjusted to fit the dynamics of Fig. 4. The values of $\gamma_a, \gamma_b, \eta_{max}$ and η_h were adjusted to fit the curves in Fig. 5. The values for g_h were adjusted to fit the hyperpolarization sag of the traces in Fig. 4. The resultant values were $V_f = -74$ mV, $g_{h_{max}} = 200$, $k = 3$ and $\tau_h = 50$ ms.

For rods, α_{cGMP}, β_{cGMP} and γ were set having in consideration two contraints: experimental results as shown in Fig. 3 and a potential of -50 mV at dark. The first time constants were then adjusted to fit the dynamics of Fig. 2. The values for g_h were adjusted to fit the hyperpolarization sag of the traces in Fig. 2. The resultant values were $V_f = -85$ mV, $g_{h_{max}} = 90$, $k = 5$ and $\tau_h = 100$ ms.

[1] td is troland, the unit of conventional retinal illuminance, and is defined as the product of the area of the pupil in mm^2 and the incident luminance in cd/m^2

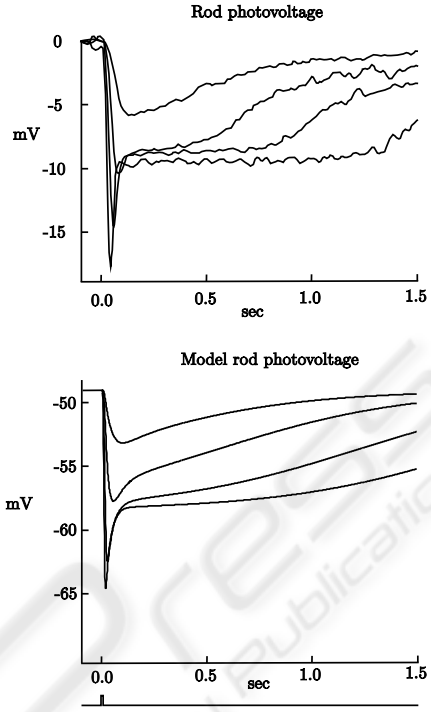

Figure 2: Rods flash response. *Top figure* shows rods flash response with resting potential set to zero, taken from (Schneeweis and Schnapf, 1999). Flash photon densities were, from top to bottom trace, 38, 140, 626.6, and 2301 photons μm^{-2}. Flash duration was 10 ms. *Bottom figure* shows rods flash responses from model. Flash strengths were, from top to bottom curve, 29.2, 107.7, 482, and 1770 td. Flash duration was 10 ms.

4 RESULTS

4.1 Rods

A rod response to an impulse (10 ms) of light usually lingers more than 1 sec. Fig. 2 shows the resemblance between real and model rods.

(Baylor et al., 1984) constructed flash-response curves (peak *current* response to different flash strengths) for several rods, which are depicted by the dots in Fig. 3. The thick continuous line is the model *voltage* flash-response curve, for the same normalized scale. The half-saturating flash strength is estimated as 50.87 td. The model curve deviates from the real response at higher intensities, probably due to the lack of adaptation mechanisms or other ionic currents in the model, but the shape of the curve is similar.

4.2 Cones

Cone voltage responses to flashes of light were acquired by (Schneeweis and Schnapf, 1999), and are

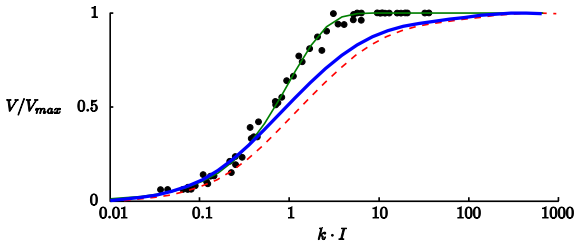

Figure 3: Rods flash-response curve. Dots represent the normalized peak *current* response of several rods to increasing 500 nm flash strengths, with 10 ms duration, taken from (Baylor et al., 1984). The thin continuous line is the expression $1-\exp(-k \cdot I)$. The thick continuous line is the model *voltage* flash-response curve, for the same normalized scale. The horizontal scale is centered at $1/k = I_0/\ln 2$, where I_0 is the half-saturating flash strength. I_0 is estimated to be 50.87 td, according to the conversion from photon density (photons μm^{-2}) to retinal illuminance (td) at 500 nm. The dashed curve is the same as the continuous curve, but as if the center of the horizontal scale was I_0 instead of $I_0/\ln 2$.

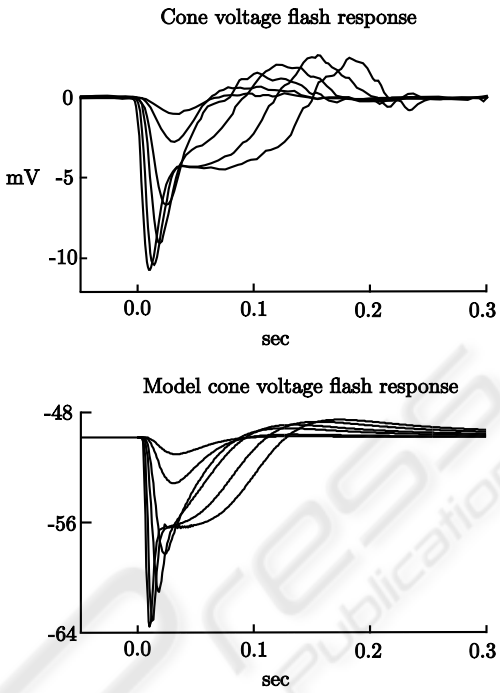

Figure 4: Cones flash responses. Top traces are voltage responses from a red cone receiving minimal input from rods, to 10 ms flashes, with photon densities ranging from 3.68×10^3 to 2.96×10^6 photons μm^{-2}, taken from (Schneeweis and Schnapf, 1999, Fig. 1). Bottom traces are voltage responses from model cones, to 10 ms flashes, with strengths (top to bottom) 600, 1200, 6×10^3, 24×10^3, 126×10^3, 482×10^3 td. The traces were taken with no input to rods, in the dark.

reproduced here in the top traces of Fig. 4. The bottom traces are voltage responses from the model cones to flashes of the same duration. The overall characteristics of the response curves are captured by the model. Namely, the sag after the peak is derived by the hyperpolarization-activated current, the sustained portion increasing with flash strength is derived from the saturation of cGMP to the lower limit, and the final overshoot is caused by the return of light adaptation effect to its resting value.

(Valeton and van Norren, 1983) stated that normalized cone peak voltage response V to steps of light in monkeys follows Michaelis-Menten equation

$$V = \frac{I^n}{I^n + \sigma^n}, \qquad (14)$$

where I is the incident light (in td), σ is the half-saturation parameter, and with $n = 0.74$. Along with increasing background intensity, this curve shifts in the intensity and the response axis. The experimental results that provided this conclusion are expressed by the dots in Fig. 5. The same figure shows the curves extracted from the model, for background intensities ranging from dark to 6 log td. The curves follow a similar response as the Michaelis-Menten equation and they are shifted in the intensity and response axis with increasing background intensity. The shift in the intensity axis is caused by the PDE activation rate reduction with decreasing calcium concentration (Eq. 4). The shift in the response axis is actually caused by two effects: to step intensities below the background intensity, the expansion of the contrast-response curve is caused by guanylate cyclase (GC) activity disinhibition with decreasing calcium concentration (Eq. 4); to step intensities above the background intensity, the hyperpolarization-activated current (I_h) compresses the response. In detail, the latter effect compresses the response because, with background light, the hyperpolarized steady potential caused by the reduction in light-sensitive current is already counteracted by the depolarization caused by the I_h current, limiting the lower value that the contrast-response can reach to a step of light.

The sensitivity of cones to steps of light reduces as ambient light increases, mainly because an increment in ambient light is not accompanied by the same increment in the derivative of the steady-state response curve. If no adaptation existed (with the exception of pigment bleaching), cone sensitivity would be described by the dot-dashed curve in Fig. 6. The dots in the same figure are data extracted by (Schnapf et al., 1990) from 4 monkey cones. Light adaptation retards the decrease in sensitivity by shifting the contrast-response curve to higher luminance levels, as shown in Fig. 5, and preventing the cone from saturating. The result from the model is shown in the thicker continuous curve in Fig. 6 and adjusts very well to experimental results. Nevertheless, the mean inten-

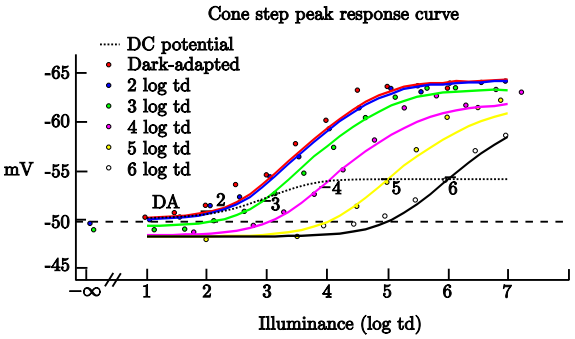

Figure 5: Cones contrast-response curves for several background light levels. The continuous curves are contrast-response curves for background intensities of (left to right) dark, 2, 3, 4, 5 and 6 log td. The dotted curve is the steady-state potential of cones versus background illuminance. The steps had 150 ms duration.

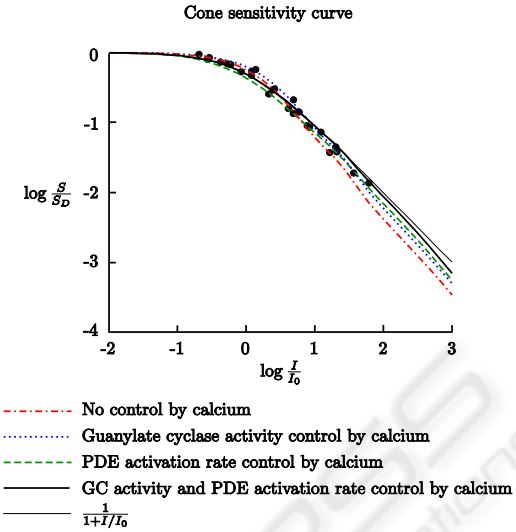

Figure 6: Cones sensitivity curve. Dots are the sensitivity to 10 ms flashes of dim light at increasing background intensities, taken from (Schnapf et al., 1990, Fig.8). Values are normalized against sensitivity in the dark S_D (vertical axis) and against the intensity I_0 that halves the sensitivity (horizontal axis). The thin continuous curve is the trace of Weber-Fechner equation $\frac{1}{1+I/I_0}$. Dot-dashed curve is the model cone sensitivity without biochemical adaptation (Ca^{2+} fixed at its value in the dark). Dotted and dashed curves are sensitivity curves with only GC activity and PDE activation rate, respectively, controled by calcium. Thick continuous curve is the model cone sensitivity with adaptation. The traces were taken with 10 ms flashes, 10% contrast, no inputs to rods, after the steady-state response has stabilized for each background intensity, with bleaching active.

sity I_0 that halves the sensitivity for the 4 cones in (Schnapf et al., 1990) was 3.3 log td, as opposed to just 2.8 log td in the model. It could be that the discrepancy relies in the fact that four cones are not representative of a population. Calcium-dependent adaptation contributes only a small portion to the overall sensitivity curve (difference between dot-dashed and thick continuous curve). It is pigment bleaching that contributes to most of the adaptation and to a linear relation between light intensity and sensitivity (also known as Weber's law) at higher intensities.

5 CONCLUSIONS

The model simulates the transduction of cones and rods, reproducing the most characteristic features. It also simulates light adaptation in cones, through photoreceptor bleaching and biochemical adaptation. It results in similar impulse response, contrast-response and sensitivity curves of monkey cones and rods.

The model is based on simple equations, never exceeding divisions and exponents. Most of the equations are sigmoidal, which may have a direct simple equivalent in semiconductor technology. The conductance-based model of the neuron is also a model with a direct equivalence to an electric circuit.

The biochemical adaptation mechanism, as well as the equations derived from it, were taken from non-primate experiments (Fain et al., 2001; Koutalos and Yau, 1996). Nonetheless, the data apparently show that the same mechanism is in effect in primates.

Additionally, several aspects have been ignored in the model, for the sake of simplicity. Firstly, the spectral sensitivity of photoreceptors was neglected, since the pathway to be realized in posterior work is achromatic (the magnocellular pathway). Secondly, the adaptation mechanism was not replicated in rods, because adaptation data and the most relevant levels of light (mesopic and photopic) relate to cones. Thirdly, the spatial dimension, although being essencial in future work where a network of cells will be simulated, is avoided in this part due to its irrevelance.

In fact, by considering the definite model as a network of photoreceptors, the set of parameters was chosen to be fixed and all results were extracted with that set. The fixed parameters are to be used as a reference set for all photoreceptors in the network, while allowing variations in turn of that set for each individual unit to create a more realistic pattern.

The adaptation mechanisms presented here are similar to the ones presented by van Hateren (van Hateren, 2005; van Hateren and Snippe, 2007): both have a calcium loop and pigment bleaching. Despite that, the formulae are substantially different, because this work was aimed to reduce the complexity of computation, with the side effect of detering more ac-

curate results. Besides, compared data is different, on account of different sites of comparison (photoreceptors in this paper, while van Hateren analyzes responses of horizontal cells).

This paper illustrates part of research with the purpose to develop a full silicon retina. Continuing research is aimed to the simulation of the outer and inner retina. The outer retina will introduce computation of spatial contrast via surround antagonism. It is expected that the inner retina discriminates object from background motion and segments objects with different motion patterns.

ACKNOWLEDGEMENTS

This work was supported by Fundação para a Ciência e Tecnologia (FCT) doctoral grant SFRH / BD / 37273 / 2007 to H.R.G..

REFERENCES

Bader, C. R., Bertrand, D., and Schwartz, E. A. (1982). Voltage-activated and calcium-activated currents studied in solitary rod inner segments from the salamander retina. *Journal of Physiology*, Vol. 331:253–284.

Baylor, D. A., Hodgkin, A. L., and Lamb, T. D. (1974). Reconstruction of the electrical responses of turtle cones to flashes and steps of light. *The Journal of Physiology*, 242(3):759–791. PMC1330661.

Baylor, D. A., Nunn, B. J., and Schnapf, J. L. (1984). The photocurrent, noise and spectral sensitivity of rods of the monkey macaca fascicularis. *The Journal of Physiology*, 357(1):575–607.

Fain, G. L., Matthews, H. R., Cornwall, M. C., and Koutalos, Y. (2001). Adaptation in vertebrate photoreceptors. *Physiol. Rev.*, 81(1):117–151.

Hodgkin, A. L. and Huxley, A. F. (1952). A quantitative description of membrane current and its application to conduction and excitation in nerve. *The Journal of Physiology*, 117(4):500–544. PMC1392413.

Hornstein, E. P., Verweij, J., Li, P. H., and Schnapf, J. L. (2005). Gap-Junctional coupling and absolute sensitivity of photoreceptors in macaque retina. *J. Neurosci.*, 25(48):11201–11209.

Koutalos, Y. and Yau, K. W. (1996). Regulation of sensitivity in vertebrate rod photoreceptors by calcium. *Trends in Neurosciences*, 19(2):73–81.

Mahroo, O. A. R. and Lamb, T. D. (2004). Recovery of the human photopic electroretinogram after bleaching exposures: Estimation of pigment regeneration kinetics. *Journal of Physiology*, 554(2):417–437.

Masland, R. H. (2001). The fundamental plan of the retina. *Nat Neurosci*, 4(9):877–886.

Perlman, I. and Normann, R. A. (1998). Light adaptation and sensitivity controlling mechanisms in vertebrate photoreceptors. *Progress in Retinal and Eye Research*, 17(4):523–563.

Rushton, W. A. H. and Henry, G. H. (1968). Bleaching and regeneration of cone pigments in man. *Vision Research*, 8(6):617–631.

Schnapf, J. L., Nunn, B. J., Meister, M., and Baylor, D. A. (1990). Visual transduction in cones of the monkey macaca fascicularis. *The Journal of Physiology*, 427(1):681–713.

Schneeweis, D. M. and Schnapf, J. L. (1999). The photovoltage of macaque cone photoreceptors: Adaptation, noise, and kinetics. *J. Neurosci.*, 19(4):1203–1216.

Soo, F. S., Detwiler, P. B., and Rieke, F. (2008). Light adaptation in salamander L-Cone photoreceptors. *J. Neurosci.*, 28(6):1331–1342.

Valeton, J. M. and van Norren, D. (1983). Light adaptation of primate cones: an analysis based on extracellular data. *Vision Research*, 23(12):1539–1547. PMID: 6666056.

van Hateren, H. (2005). A cellular and molecular model of response kinetics and adaptation in primate cones and horizontal cells. *Journal of Vision*, 5(4):331–347.

van Hateren, J. H. (2007). A model of spatiotemporal signal processing by primate cones and horizontal cells. *Journal of Vision*, 7(3):1–19.

van Hateren, J. H. and Snippe, H. P. (2007). Simulating human cones from mid-mesopic up to high-photopic luminances. *Journal of Vision*, 7(4).

Verweij, J., Hornstein, E. P., and Schnapf, J. L. (2003). Surround antagonism in macaque cone photoreceptors. *J. Neurosci.*, 23(32):10249–10257.